THE JOURNAL OF PHYSICAL CHEMISTRY Letters

Letter

pubs.acs.org/JPCL

Interaction of NH_3 with Cu-SSZ-13 Catalyst: A Complementary FTIR, XANES, and XES Study

Filippo Giordanino,[†,‡] Elisa Borfecchia,[†,‡] Kirill A. Lomachenko,[†,#] Andrea Lazzarini,[†,‡] Giovanni Agostini,[∥] Erik Gallo,[∥] Alexander V. Soldatov,[#] Pablo Beato,[⊥] Silvia Bordiga,*[,†,‡] and Carlo Lamberti[†,§,#]

[†]Department of Chemistry and INSTM Reference Center, [‡]NIS Centre of Excellence, and [§]CrisDI Center of Crystallography, University of Turin, via P. Giuria 7, 10125 Turin, Italy

[∥]European Synchrotron Radiation Facility, 6, rue Jules Horowitz, B.P. 220, F-38043 Grenoble cedex, France

[⊥]Haldor Topsøe A/S, Nymøllevej 55, 2800 Kgs. Lyngby, Denmark

[#]Southern Federal University, Zorge street 5, 344090 Rostov-on-Don, Russia

Supporting Information

ABSTRACT: In the typical NH_3–SCR temperature range (100–500 °C), ammonia is one of the main adsorbed species on acidic sites of Cu-SSZ-13 catalyst. Therefore, the study of adsorbed ammonia at high temperature is a key step for the understanding of its role in the NH_3–SCR catalytic cycle. We employed different spectroscopic techniques to investigate the nature of the different complexes occurring upon NH_3 interaction. In particular, FTIR spectroscopy revealed the formation of different NH_3 species, that is, (i) NH_3 bonded to copper centers, (ii) NH_3 bonded to Brønsted sites, and (iii) $NH_4^+ \cdot nNH_3$ associations. XANES and XES spectroscopy allowed us to get an insight into the geometry and electronic structure of Cu centers upon NH_3 adsorption, revealing for the first time in Cu-SSZ-13 the presence of linear Cu^+ species in O_{fw}–Cu–NH_3 or H_3N–Cu–NH_3 configuration.

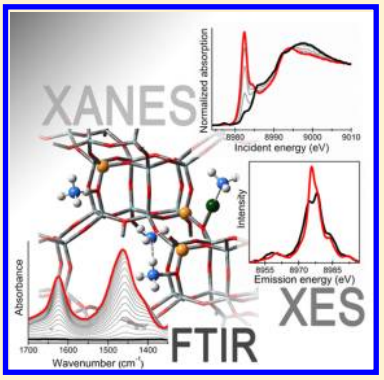

SECTION: Surfaces, Interfaces, Porous Materials, and Catalysis

The selective catalytic reduction with ammonia (NH_3–SCR) is an effective way to remove hazardous NO_x compounds from automotive gas emissions.[1−4] Among the various catalysts tested for this purpose, copper-containing zeolites showed high performance over a wide range of temperatures and conditions. In particular, because of its superior thermal stability, small-pore Cu-SSZ-13 zeolite has been recently selected as a promising candidate for commercial applications.[1,5−7] During the past few years, an impressive number of papers appeared in the literature aiming to clarify the catalytic cycle of the NH_3–SCR reaction over Cu-zeolites,[1−8] but up to now, a clear picture is still missing.

Traditionally, on the basis of previous study on vanadia catalyst,[2] two main NH_3–SCR mechanisms have been proposed over Cu-zeolites: in the Langmuir–Hinshelwood mechanism, the interaction between adsorbed NH_3 and surface nitrite and nitrate is thought to be the key step of the reaction;[8,9] conversely, in the Eley–Rideal mechanism, gas-phase NO_2 interacts with two adjacent NH_4^+ ions to form a $(NH_4)_xNO_2$ complex.[2] Both mechanisms are based on the fact that first NO needs to be oxidized to NO_2 (or directly converted to nitrate/nitrite species), which can be further reduced to N_2 and H_2O.[2] Recently, Gao et al.[1] proposed a new low-temperature mechanism where they claim the importance of the NH_3–Cu^+–NO^+ complex formation as an alternative way to the initial NO oxidation step. Contextually, Ruggeri et al. stated that the oxidation of NO to NO_2 as a rate-determining step of the standard SCR reaction is remarkably questionable.[10] In all reported mechanisms, adsorbed NH_3 species play a crucial role because they act as reducing agent of NO. Hence, the study of the interaction between the catalyst and NH_3 is fundamental. FTIR spectroscopy is a powerful technique in catalysis,[11−13] which has been successfully employed to identify different kind of adsorbed ammonia species involved in the SCR catalytic cycle.[14−17] Commonly, two types of adsorbed NH_3 could be easily detected by infrared spectroscopy: (i) NH_3 coordinated to Lewis acid sites (Cu sites, extraframework Al^{3+}), with the formation of corresponding amino complexes that usually give rise to an absorption band at ∼1620 cm^{-1} associated with $\delta_{as}(NH)$ mode (corresponding $\delta_s(NH)$ mode usually lies at frequencies lower than 1250 cm^{-1}, becoming overshadowed by the high intensity modes of the zeolitic structure) and (ii) NH_3 interacting with residual bridged hydroxyls groups, that is,

Received: February 4, 2014
Accepted: April 10, 2014
Published: April 10, 2014

   dx.doi.org/10.1021/jz500241m | J. Phys. Chem. Lett. 2014, 5, 1552−1559

Brønsted acid sites, with the formation of NH_4^+ ions and the appearance of corresponding signals in the 1500−1350 cm^{-1} range. In the latter case, the occurrence of solvated NH_4^+ species, that is, $NH_4^+ \cdot nNH_3$ ($n \geq 1$), is also possible, depending on temperature and NH_3 coverage.[18−20]

FTIR spectroscopy of adsorbed NH_3 is able to provide a comprehensive view on the different NH_3-adsorbed species, allowing their identification. However, the technique lacks sensitivity in the electronic and geometric properties of the adsorbing site, which could be crucial to obtain further insights into the SCR mechanism. Conversely, direct information on the local coordination geometry and electronic properties of the Cu sites can be accessed by XAS and XES spectroscopies, exploiting the element selectivity of the techniques.[21−23] XAS has already been employed in the characterization of the Cu-SSZ-13 zeolite to clarify the local coordination environment of the metal sites in the calcinated material[24] and to monitor its evolution in SCR-relevant conditions.[4,25,26] These studies related the high catalytic performance of Cu-SSZ-13 to the presence of isolated mononuclear Cu^{2+} species in the zeolite cavities. Indeed, the band at 22 700 cm^{-1} (440 nm) in the UV−vis and the Raman bands at 270, 455, and 870 cm^{-1} (that undergo Raman enhancement when excited with the 488 nm laser), observed in Cu-ZSM-5,[27] are not present in this Cu-SSZ-13 sample.[28]

Because the complexity of the interaction between the Cu centers and the reactants under SCR-conditions, it is difficult to unambiguously distinguish the role of each gas feed component in the reaction mechanism and to identify the principal intermediates species. Hence, it is important to separately investigate the interaction of each reactant with the catalyst. However, to the best of our knowledge, no previous XAS or XES studies focused on the adsorption of NH_3 on Cu-SSZ-13 have been reported in the literature, although they are indispensable to clarify the local atomic and electronic structure of the resulting species. Here we report a multitechnique investigation of the NH_3 interaction with the Cu-SSZ-13 catalyst, combining FTIR spectroscopy, sensitive to the different NH_3 adsorption sites in the zeolite, and XAS/XES methods, which provide selective information on the NH_3 coordination to the Cu sites relevant for the SCR reaction.

Prior to ammonia adsorption, the sample needs to be dehydrated; it is well-known that dehydration process modifies the initial oxidation state of copper depending on the type of activation conditions. XANES measurements were performed to characterize the Cu-SSZ-13 samples activated in vacuo and in O_2/He flux to appreciate the differences in the oxidation state and the local coordination geometry of Cu centers. Figure 1 reports the XANES spectra of Cu-SSZ-13 in its hydrated state collected at room temperature (blue curve) and after activation at 400 °C performed both in O_2/He flux (black curve) and in vacuo (green curve). The XANES spectrum of the hydrated Cu-SSZ-13 shows the typical features of hydrated Cu^{2+} ions,[29,30] in accordance with previous literature on Cu-zeolites prepared by aqueous ion exchange.[26,31−34]

In particular, a weak pre-edge peak **A** is clearly observed at ∼8977.3 eV. This transition is conventionally assigned to 1s → 3d transition in Cu^{2+}.[34−38] However, a minor 1s → 4p contribution is also expected to be involved. In addition, for the hydrated sample, a high-intensity white line feature **D** is present at ∼8995.3, typical of Cu^{2+} centers in a highly coordinated form, for example, when the coordination sphere of the cation is saturated by water molecules or by a combination of framework oxygens, water molecules, and, eventually, OH groups.[33]

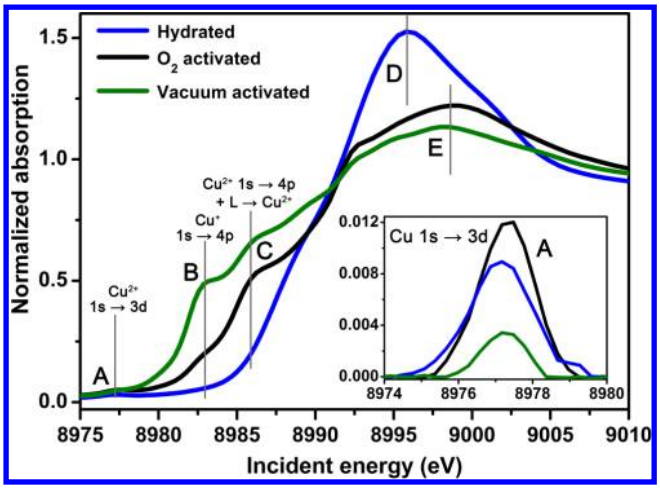

Figure 1. Cu K-edge XANES spectra of Cu-SSZ-13 in its hydrated state (blue curve) collected at room temperature and after the activation process at 400 °C, performed in both in vacuo conditions (green curve) and O_2/He flux (black curve). The principal XANES features are labeled with the **A**−**E** letters, and the inset reports a magnification of the background-subtracted XANES spectra in the region where the weak Cu^{2+} 1s → 3d peak (**A**) is observed.

It is worth noting that the **A** transition is not present in Cu^+ complexes due to their d^{10} configuration.[34] Thus, it can be employed to fingerprint the presence of Cu^{2+} and qualitatively evaluate its abundance in the investigated samples by examining the background subtracted intensity of the correspondent pre-edge peak. Nonetheless, it has been shown that the intensity and the shape of the **A** feature are also influenced by the symmetry of the local Cu^{2+} coordination environment and therefore by the level of 3d−4p orbital mixing.[36,39] Hence, more reliable information on the Cu oxidation state is obtained by considering the intensity of peak **A** in conjunction with the other relevant XANES features.

Upon in vacuo heating from RT to 400 °C, a clear evolution of the XANES feature is observed. Finally, for vacuum-activated Cu-SSZ-13 sample, the intensity of feature **A** is significantly reduced with respect to the hydrated sample, although a residual peak is still present. In addition, the white line resonance **D** shifts at higher energy (at ∼8998.6 eV, peak **E**) and two main transitions appear in the pre-edge region: a distinct peak **B** at ∼8982.8 eV and a shoulder **C** at ∼8986.3 eV.

Interestingly, XANES spectra for Cu^+ systems are commonly characterized by distinct pre-edge features in the 8982−8985 eV range, whereas for the Cu^{2+} species, pre-edge peaks below 8985 eV are mostly not observed,[35] except for the 1s → 3d transition previously discussed. According to this general trend, feature **B** is assigned the 1s → 4p transition of Cu^+.[34,35,40,41] The energy position of this feature, in the 8982−8984 eV range, is typical of two- or three-coordinated Cu^+ sites.[35,38] This assignment, in combination with the significant decrease in the intensity of feature **A**, strongly suggests that vacuum activation induces the "self reduction" of a substantial fraction of the initial Cu^{2+} sites to Cu^+, as previously reported, for example, for the Cu-ZSM-5 zeolite.[41,42]

Nevertheless, the reduction is not total, and a minor contribution from Cu^{2+} sites is still present, as demonstrated by the persistence of feature **A**. This was the case of Cu-MOR activated under the same conditions,[34] while a virtually total

dx.doi.org/10.1021/jz500241m | J. Phys. Chem. Lett. 2014, 5, 1552−1559

reduction to Cu^+ was observed for Cu-ZSM-5.[42] This evidence is also supported by the presence of the shoulder **C**, assigned to the Cu^{2+} 1s → 4p + ligand (L) and to the Cu^{2+} 1s → Cu^{2+} charge-transfer excitation,[43] similarly to what is observed in the planar $Cu(OH)_2$ complex[38] and already observed in activated Cu-SSZ-13.[25,26] It is, however, worth noting that a complete reduction of the Cu^{2+} centers could be reached by increasing the activation time, as was recently demonstrated by Giordanino et al.[28] using FTIR spectroscopy.

The overall shape of the XANES spectrum for the O_2-activated Cu-SSZ-13 is quite similar to that observed for vacuum-activated sample, previously discussed. This analogy reflects the similarity in the local coordination environment of the Cu centers after the two different activation processes, resulting in oxygen-coordinated monomeric species isolated in the zeolite framework. However, two key differences are observed, which point out significant variations in Cu oxidation state after O_2 and vacuum activation: (i) for the O_2-activated Cu-SSZ-13, a slight enhancement in the intensity of feature **A** with respect to the hydrated material is observed, as expected due to the lowering in Cu^{2+} coordination symmetry upon dehydration and increased interaction with the zeolite framework;[34,36,39,42] (ii) the pre-edge region for the O_2-activated sample is dominated by feature **C**, typical of Cu^{2+} centers, while the **B** peak, diagnostic for the Cu^+ presence, is remarkably less intense with respect to the one found after vacuum activation.

This evidence demonstrates that the O_2 activation is effective in limiting the "self reduction" process[34,42] in Cu-SSZ-13 and results in a majority of Cu^{2+} sites, with a minor contribution from reduced Cu^+ centers.

Because an oxidative activation reflects the real working condition of the catalyst,[44] hereinafter we mainly focus on the NH_3 adsorption on O_2-activated sample, which contains a majority of Cu^{2+} centers, as follows from the XANES analysis.

Ammonia (PA = 853.5 kJ mol^{-1}) is known as typical strong base.[45] The kinetic diameter of ammonia based on the Lennard-Jones relationship is 2.6 Å. Because the diameter of 8MR of the CHA structure is ~3.8 Å, an ammonia molecule reaches almost all acid sites, that is, Lewis and Brønsted sites in zeolites.

Figure 2 shows the infrared spectra recorded on the O_2-activated sample during the exposure to ammonia at 100 °C. Starting from low ammonia coverage, a gradual consumption of the 3611 and 3584 cm^{-1} bands related to ν(OH) of bridged hydroxyls with a strong Brønsted acidity[46] is observed.

It is worth noting that, as also previously observed by Lezcano-Gonzalez et al.,[17] the intensity of the bands related to ν(OH) modes of Brønsted sites is surprisingly high and quite comparable to the parent material H-SSZ-13. This is an interesting evidence because the intensity of these bands should decrease consistently in a sample characterized by a Cu/Al ratio of 0.444. In particular, it is commonly assumed that when copper is introduced in the zeolitic framework upon aqueous ion exchange, the positive charge (+2) of Cu^{2+} ions must be balanced by two negative charges, likely represented by two aluminum atoms in close proximity. Therefore, a ratio of Cu/Al = 0.5 should represent the total ion exchange level. Conversely, our results clearly show that a consistent concentration of not exchanged sites, that is, Brønsted sites, is still present even if the Cu/Al ratio is not far from the stoichiometric exchange level. This is a novel evidence that suggests that likely, during the exchange procedure, part of Brønsted sites are exchanged by monovalent copper complexes, such as $[CuOH]^+$.[28] Further studies would be required to clarify this point, possibly allowing us to revisit the nature of the Cu sites in the activated catalyst.

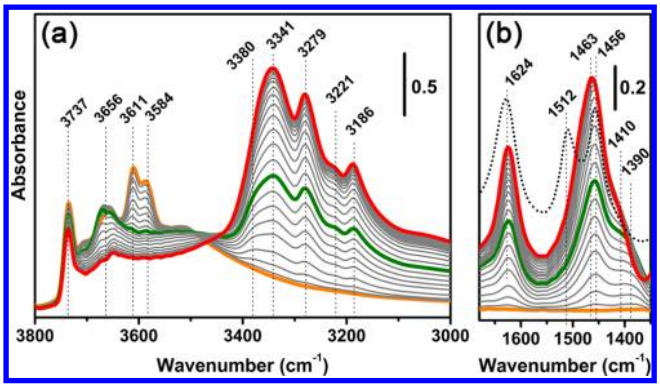

Figure 2. FTIR spectra of Cu-SSZ-13 at increasing contact time with 1800 ppm of NH_3/He mixture (100 °C). Spectra are reported in both ν(NH) (panel a) and δ(NH) (panel b, spectra reported after the subtraction of the spectrum of the dehydrated zeolite sample) regions. Orange curve refers to activated sample, red curve refers to highest contact time, that is, highest ammonia loading, and gray curves relate to intermediate ammonia loadings. Green curve refers to the total consumption of Brønsted sites. Dotted black curve in panel b refers to the spectrum of Cu-SSZ-13 upon NH_3 adsorption at room temperature.

The FTIR bands related to ν(OH) of bridged hydroxyls with a strong Brønsted acidity totally disappear when $NH_3/H^+ = 1$ (green curve). Simultaneously, complex absorption features develop in the 1550−1350 cm^{-1} region, showing two main component at 1456 and 1380 cm^{-1}, which shift to higher wavenumbers for $NH_3/H^+ > 1$, together with the appearance of new features in the 3400−3100 cm^{-1} range. These bands are commonly associated with the δ(NH) and ν(NH) modes, respectively, of NH_4^+ ion formed upon NH_3 protonation by Brønsted acidic hydroxyls groups.[18] Concurrently to the formation of NH_4^+ ions, the interaction of NH_3 with Lewis copper sites is confirmed by the appearance of the band at 1624 cm^{-1}.[14] It is important to note that also the presence of extra-framework Al (EFAl) could give a contribution at the same frequency.[17] This band was not observed on H-SSZ-13 zeolite activated under the same conditions of Cu-SSZ-13 (see Supporting Information, Figure S1); in addition, ^{27}Al MAS SSNMR spectrum of H-SSZ-13 (see Supporting Information, Figure S4) reveals a concentration of octahedral-like Al species lower than 5%, excluding the presence of a significant fraction of EFAl species in the samples under investigation. Moreover, the 1624 cm^{-1} band could be associated with molecular ammonia bonded on both Cu^+ and Cu^{2+} sites; indeed, the band does not change in intensity and position if ammonia is dosed on both vacuum and O_2-activated samples (see Supporting Information, Figure S2), where a prevalence of Cu^+ and Cu^{2+} centers is expected, respectively.[28]

The fact that 1550−1350 and 1624 cm^{-1} features develop together suggests similar adsorption energy of the two acidic sites. A gradual but not total consumption of 3737 cm^{-1} band is also observed due to the interaction of ammonia with the silanols prevalently located on external surfaces of the catalyst. Additionally, the band at 3656 cm^{-1} that we recently associated with $[Cu^{2+}OH^-]^+$ sites[28] is also eroded, indicating that ammonia could be adsorbed even on these particular sites. It is worth noting that this band is consumed only after the saturation of all Brønsted sites ($NH_3/H^+ = 1$).

dx.doi.org/10.1021/jz500241m | J. Phys. Chem. Lett. 2014, 5, 1552−1559

The nature of ammonia complexes in H-form zeolites has been studied by Zecchina et al.[18] The authors revealed that, at room temperature, in H-ZSM-5, H-BEA, HY, and H-SAPO-34, framework oxygens stabilize mostly bidentate and tridentate ammonium ions. In particular, the triple degeneracy of the ν_4 mode of the "free" NH_4 ions (T_d symmetry) is removed due to the H bonding, leading to an absorption feature in the 1550−1350 cm^{-1} region. Because the frequency of these bands can change depending on symmetry or different adsorption sites, it can be expected that ν_4 bands of the NH_4^+ ions appear as a featureless and broad band. As reported in Figure 3c, the

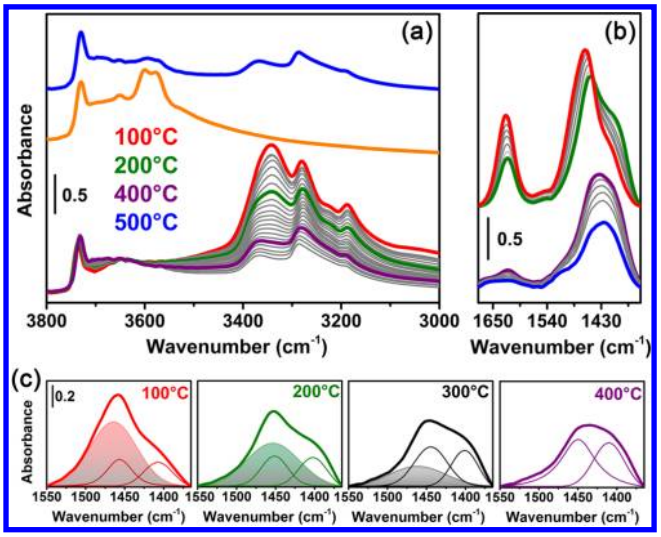

Figure 3. Helium NH_3-temperature-programmed desorption (TPD) over Cu-SSZ-13 followed by FTIR in the 100−500 °C temperature range. Spectra are reported in both ν(NH) (panel a) and δ(NH) (panel b, spectra reported after the subtraction of the spectrum of the dehydrated zeolite sample) regions. Gray curves refer to spectra recorded at intermediate temperature. In panel a, the spectrum of dehydrated sample is also reported (orange curve). Panel c shows the deconvoluted δ(NH) spectra of NH_4^+ ions at different desorption temperature. Filled area refers to $NH_4{\cdot}nNH_3$ associations band observed at 1460 cm^{-1}. The two other components at 1450 and 1400 cm^{-1} refer to the antisymmetric and symmetric bending vibrations of NH_4^+.

deconvoluted spectrum of the NH_4^+ ions recorded at 100 °C shows three main components at 1463, 1456, and 1406 cm^{-1}. Lónyi et al.[20] observed similar bands dosing NH_3 on acidic porous materials. The authors stressed the fact that the component bands resolved in the 1550−1300 cm^{-1} region cannot be assigned to the ν_4 modes of a single H-bonded NH_4^+ species but to overlapping bands of NH_4^+ ions H-bonded to various extent in $NH_4^+{\cdot}nNH_3$ associations ($n \geq 1$). Indeed, it is expected that for $NH_4^+/H^+ > 1$ the coordination of ammonia to NH_4^+ ions leads the formation of $NH_4^+{\cdot}nNH_3$ species. In particular, it has been observed that H-bonding of NH_3 to the zeolite-bonded NH_4^+ ions shifts the ν_4 bands of the ion at higher wavenumbers of an extent likely dependent on the number of NH_3 molecules, that is, n value, which solvate the NH_4^+ ions.[20] With this respect, the last statement is supported by the appearance of the highly blue-shifted band at 1512 cm^{-1} (dotted black curve in Figure 2b) that we observe after adsorption of high partial pressures of NH_3 at room temperature. A similar band was observed by other authors,[20,47] and it has been associated with a bending vibration of NH_4^+ species H-bonded to NH_3. The absence of the well-resolved band at 1512 cm^{-1} in the other spectra reported in Figure 2b does not exclude the occurrence of $NH_4^+{\cdot}nNH_3$ associations at 100 °C. Indeed, spectra collected at this temperature are characterized by bands at 1700 and 2770 cm^{-1} (see Supporting Information, Figure S3), which have been assigned to bending mode of molecular ammonia coordinated to NH_4^+ ions and to N−H stretching mode of NH_4^+ ions H-bonded to NH_3.[18,48]

The changes in the infrared spectra recorded during the NH_3 desorption process (Figure 3) allowed us to study the thermal stability of different ammonia species and better investigate the complex band contributions due to $NH_4^+{\cdot}nNH_3$ associations in the 100−500 °C temperature range. In the bending region (Figure 3b), the desorption process is accompanied by a gradual intensity decrease in the band at 1624 cm^{-1}, which totally disappears at 500 °C, indicating that at this temperature ammonia-bonded to copper sites is completely desorbed. Conversely, the complex signal related to protonated ammonia is still persistent at 500 °C, suggesting a high thermal stability of these species with comparison to NH_3 bonded on copper sites. This is likely related to the stabilization of the NH_4^+ ions via H-bonding to the framework oxygens. Starting from 100 °C, the evolution of the NH_4^+ signal during the desorption process could be ascribed as follows: the intensity decrease, and the red shift of the component at 1463 cm^{-1} is accompanied in the 100−400 °C temperature range by the growth in intensity of the component at around 1400 cm^{-1}, which evolves at high temperature in a unique broad band centered at 1430 cm^{-1}; this behavior clearly indicates that during the desorption process the species associated with the band at 1463 cm^{-1} are transformed into the species related to the 1430 cm^{-1} band. This is supported by the observed isosbestic point at 1440 cm^{-1}. Taking into account the fact that the solvation effect shifts the vibration modes of NH_4^+ ions to higher wavenumbers, as evidenced by the appearance at room temperature of the band at 1512 cm^{-1} (see Figure 2b), the band at 1463 cm^{-1} could be still considered a manifestation of $NH_4^+{\cdot}nNH_3$ associations. It is, however, important to note that at 100 °C n value is likely lower than room temperature due to the fact that an increased temperature could limit the amount of solvating NH_3 molecules. Deconvoluted spectra[49] at different desorption temperature (Figure 3c) show that the 1430 cm^{-1} band is composed of two main components at 1450 and 1400 cm^{-1}, which rise in intensity at the expense of the band at 1463 cm^{-1}: these two bands could be easily assigned to the antisymmetric and symmetric bending vibrations of not-solvated NH_4^+ ions, respectively.[17] In the 400−500 °C temperature range, the 1430 cm^{-1} band decreases in intensity, while the intensity of the signals at 3611 and 3584 cm^{-1} is partially restored; contemporaneously, the bands in the 3400−3100 cm^{-1} range decrease in intensity, shifting to higher wavenumbers at high temperature (Figure 3a). On the basis of these observations, one can conclude that the desorption of solvating ammonia molecules from $NH_4^+{\cdot}nNH_3$ associations (likely represented by the band at 1463 cm^{-1}) leads to not-solvated NH_4^+ ions (characterized by deconvoluted components at ν_{as} = 1450 cm^{-1} and ν_s = 1430 cm^{-1}), which can further decompose for $T > 400$ °C as follow: $NH_4^+ \rightarrow NH_3 + H^+$.

Summarizing, from FTIR analysis, we identified different kind of adsorbed ammonia potentially available for SCR reaction: (i) NH_3 bonded to copper sites, that is, both isolated Cu^{2+} and $[Cu^{2+}OH^-]^+$ sites; (ii) protonated NH_3 as NH_4^+ ionic form, that is, NH_3 bonded to Brønsted sites; and (iii)

dx.doi.org/10.1021/jz500241m | J. Phys. Chem. Lett. 2014, 5, 1552−1559

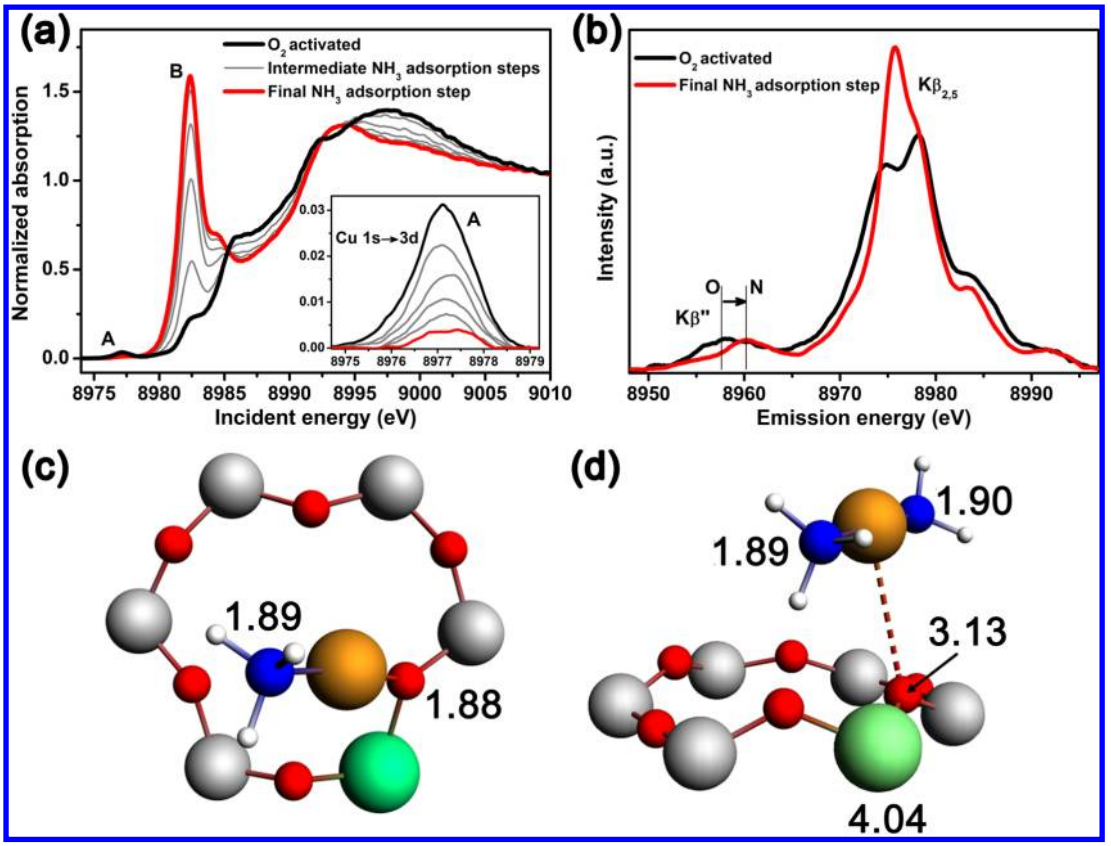

Figure 4. (a) In situ evolution of the Cu K-edge HERFD XANES spectra of O_2/He-activated Cu-SSZ-13 during the interaction with a flow of 1300 ppm of NH_3 in He at 120 °C. The inset magnifies the pre-edge region with the background subtracted. (b) Background-subtracted Cu K$\beta_{2,5}$ and Kβ'' emission lines for the initial and final stages of the process. (c,d) Cu local environment after adsorption of one and two NH_3 molecules, respectively (only the six-ring atoms are shown: the whole cluster used in the structural optimization is reported in Figure S5 of the Supporting Information). Color code: orange, Cu; green, Al; gray, Si; red, O; blue, N; white, H. Distances between Cu and neighboring atoms are indicated in angstroms.

solvated NH_4^+ ions, that is, $NH_4^+ \cdot nNH_3$ associations. Species (i) and (iii) have been found to be more stable for $T < 400$ °C, while at higher temperature species (ii) is the more abundant.

Interaction of Cu-SSZ-13 with NH_3 was also monitored in situ by K$\beta_{1,3}$ HERFD (high energy resolution fluorescence detection) XANES (Figure 4a).[22,23,50] Initial spectrum corresponds to the sample activated at 400 °C in oxygen/helium flux and is equivalent to the one presented in Figure 1. The only difference is that the pre-edge peaks are more pronounced compared with conventional XANES because of the lower level of background.[22,23,50] The high intensity of the pre-edge 1s → 3d transition **A** confirms that the copper oxidation state is close to +2. However, when ammonia is introduced in the reactor, the area of this pre-edge feature starts to decrease steadily and reaches the minimum of ∼10% of its initial value in the NH_3-saturated state at the end of the adsorption process. (See the inset of Figure 4a.) At the same time, the peak **B** at 8982.5 eV, which is characteristic for Cu^+ species,[35] rises dramatically, surpassing even the main edge maximum. This serves as a clear indication for the reduction of Cu species from Cu^{2+} to Cu^+. Moreover, such a high intensity of the peak **B** suggests a linear coordination of the Cu species.[35,51,52] Under the adopted experimental conditions, this could be either a O_{fw}−Cu−NH_3 configuration, where copper is still coordinated to one framework oxygen O_{fw}, or the H_3N−Cu−NH_3 structure, where copper forms a complex with two NH_3 molecules inside the zeolite cavity. Similar complex has already been reported in a zeolitic framework (ferrierite) and well-characterized by X-ray diffraction, as described in the study of Gomez-Lor et al.[53] In that case, the distances between copper and the nearest oxygen were 3.95 Å. The formation of a O_{fw}−Cu−O_{fw} linear species can be ruled out because the NH_3 coordination to copper is clearly evidenced by Cu X-ray emission spectra (Figure 4b). First, the significant alteration of the K$\beta_{2,5}$ line shape indicates the different local coordination geometry and symmetry in the initial and final stages of the adsorption process, as previously observed for instance on Ti silicalite-1 (TS-1) upon NH_3 adsorption.[54,55] Second, the blue shift of the Kβ'' satellite for the final product with respect to the initial stage with oxygen-only coordination proves the formation of Cu−N bond. Indeed, this peak originates from the ligand 2s to metal 1s crossover transition and is therefore sensitive to the binding energy of the ligand 2s orbital.[56,57] Because the nitrogen 2s level lies higher in energy than the one of oxygen, the coordination of the former causes the blue shift of the peak.

To support these structural findings, DFT calculations were carried out using ADF2012 package.[58,59] Geometry optimization was performed adding NH_3 molecules in the vicinity of the Cu atom placed in the d6r on the base of the previous work by Deka et al.[25] Results indicate that a single NH_3 ligand drives Cu ion outside of the d6r unit plane, forming an almost linear O_{fw}−Cu−NH_3 structure with O−Cu−N angle of 172° (Figure 4c). The second ammonia molecule lifts Cu even higher in the large cavity, while the N−Cu−N angle reaches 177° (Figure 4d). Both structures are in agreement with the XANES and XES

dx.doi.org/10.1021/jz500241m | J. Phys. Chem. Lett. 2014, 5, 1552−1559

data previously discussed. However, because of the similarity of bond distances and angles, discrimination between these two possible cases remains an ongoing challenge.

The reduction of a transition-metal center M due to NH_3 dissociative chemisorption, reaction 1, has already been proposed for oxide-based materials employed as ammonia oxidation catalysts.[60] The process involves the activation of ammonia, possibly via the amide species, which is followed by a coupling reaction that yields nitrogen as ammonia oxidation product, reaction 2:

$$NH_3 + M^{n+} + O^{2-} \rightarrow M^{(n-1)+}{-}NH_2 + (OH)^- \quad (1)$$

$$2M^{(n-1)+}{-}NH_2 \rightarrow N_2H_4 \rightarrow N_2 + 4H^+ + 4e^- \quad (2)$$

Cu-zeolites typically show a good ammonia oxidation activity at relative high temperature.[61] However, in our case, reaction 2 is supposed to be unfavored because it is improbable to find two metal centers close enough to allow the formation of N_2H_4. This is particularly true for Cu-SSZ-13 catalyst, which has been claimed to contain mainly well-dispersed isolated copper ions. Although reaction 1 is still compatible with our XAS/XES results, it is in contrast with FTIR analysis. Indeed, the formation of $-NH_2$-like groups should give rise to absorption features at around 3520, 3440, and 1550−1510 cm^{-1}, associated with ν(NH) and δ(NH) modes, respectively,[62−66] which are not observed in our spectra collected at 100 °C. (See Figure 2.) On the basis of these observations, a dissociative chemisorption of NH_3 on copper sites is unlikely, while a simple molecular coordination remains the most probable scenario. To explain the reduction of copper sites and their capability to form linear complexes as clearly demonstrated by XAS/XES, an alternative pathway needs to be proposed:

$$Cu^{2+} + e^- \rightarrow Cu^+ \quad (3)$$

$$2NH_3 \rightarrow 6H^+ + 6e^- + N_2 \quad (4)$$

In this case, NH_3 oxidation, reaction 4, represents the electron supply needed for the reduction of Cu^{2+} sites, reaction 3. In turn, Cu^+ ions could coordinate one or two NH_3 molecules, leading to the formation of linear complexes. Despite the fact that this mechanism needs to be supported by further experimental evidence, the Cu reduction observed by HERFD XANES concomitantly to NH_3 adsorption (Figure 4) has potential implications on revisiting the low-temperature SCR mechanism. Indeed, this evidence highlights the fact that coordinated NO is not the only SCR reactant able to reduce Cu^{2+}[1,67] and that a key role in the Cu^{2+}/Cu^+ redox cycle could be also played by ammonia. In addition, the observed possibility to stabilize a Cu(I) complex inside SSZ-13 zeolitic matrix could open new synthetic routes for the preparation of novel Cu-based catalyst starting from Cu(I) precursors. So far, a totally exchanged Cu zeolite system has been prepared starting from CuCl gas-phase ion exchange,[32] a way that does not guarantee the absence of chloride-like extra phases[68,69] with compromising effects on the catalytic activity of the final material. Conversely, the use of a chloride-"free" precursor, that is, Cu(I)−amino complex, could result in an enhanced purity and consequently improved performance.

■ ASSOCIATED CONTENT

Ⓢ Supporting Information

Additional FTIR spectra, ^{27}Al MAS NMR analysis, and experimental/computational details are reported.

This material is available free of charge via the Internet at http://pubs.acs.org.

■ AUTHOR INFORMATION

Corresponding Author

*E-mail: silvia.bordiga@unito.it.

Notes

The authors declare no competing financial interest.

■ ACKNOWLEDGMENTS

This work has been supported by "Progetti di Ricerca di Ateneo-Compagnia di San Paolo-2011- Linea 1", ORTO11RRT5 project. C.L., K.A.L., and A.V.S. thank the support from the Mega-grant of the Russian Federation Government to support scientific research at Southern Federal University, no. 14.Y26.31.0001. We acknowledge P. Glatzel, C. Lapras, and O. Mathon for their help during beamtime at the ID26 and BM23 beamlines, ESRF. We are also grateful to A. P. Molina for her contribution and valuable discussions during experiments performed at the ID26 beamline (ESRF) and to M. R. Chierotti and R. Gobetto for having performed ^{27}Al MAS NMR measurements.

■ REFERENCES

(1) Gao, F.; Kwak, J.; Szanyi, J.; Peden, C. F. Current Understanding of Cu-Exchanged Chabazite Molecular Sieves for Use as Commercial Diesel Engine DeNO$_x$ Catalysts. *Top. Catal.* **2013**, *56*, 1441−1459.

(2) Brandenberger, S.; Krocher, O.; Tissler, A.; Althoff, R. The State of the Art in Selective Catalytic Reduction of NO$_x$ by Ammonia Using Metal-Exchanged Zeolite Catalysts. *Catal. Rev.* **2008**, *50*, 492−531.

(3) Gabrielsson, P. L. T. Urea-SCR in Automotive Applications. *Top. Catal.* **2004**, *28*, 177−184.

(4) Deka, U.; Lezcano-Gonzalez, I.; Weckhuysen, B. M.; Beale, A. M. Local Environment and Nature of Cu Active Sites in Zeolite-Based Catalysts for the Selective Catalytic Reduction of NO$_x$. *ACS Catal.* **2013**, *3*, 413−427.

(5) Fickel, D. W.; D'Addio, E.; Lauterbach, J. A.; Lobo, R. F. The Ammonia Selective Catalytic Reduction Activity of Copper-Exchanged Small-Pore Zeolites. *Appl. Catal., B* **2011**, *102*, 441−448.

(6) Fickel, D. W.; Fedeyko, J. M.; Lobo, R. F. Copper Coordination in Cu-SSZ-13 and Cu-SSZ-16 Investigated by Variable-Temperature XRD. *J. Phys. Chem. C* **2010**, *114*, 1633−1640.

(7) Kwak, J. H.; Tonkyn, R. G.; Kim, D. H.; Szanyi, J.; Peden, C. H. F. Excellent Activity and Selectivity of Cu-SSZ-13 in the Selective Catalytic Reduction of NO$_x$ with NH_3. *J. Catal.* **2010**, *275*, 187−190.

(8) Grossale, A.; Nova, I.; Tronconi, E.; Chatterjee, D.; Weibel, M. NH_3-NO/NO$_2$ SCR for Diesel Exhausts Aftertreatment: Reactivity, Mechanism and Kinetic Modelling of Commercial Fe- and Cu-Promoted Zeolite Catalysts. *Top. Catal.* **2009**, *52*, 1837−1841.

(9) Ruggeri, M. P.; Grossale, A.; Nova, I.; Tronconi, E.; Jirglova, H.; Sobalik, Z. FTIR in Situ Mechanistic Study of the NH_3-NO/NO$_2$ Fast SCR Reaction over a Commercial Fe-ZSM-5 Catalyst. *Catal. Today* **2012**, *184*, 107−114.

(10) Ruggeri, M.; Nova, I.; Tronconi, E. Experimental Study of the NO Oxidation to NO$_2$ over Metal Promoted Zeolites Aimed at the Identification of the Standard SCR Rate Determining Step. *Top. Catal.* **2013**, *56*, 109−113.

(11) Lamberti, C.; Groppo, E.; Spoto, G.; Bordiga, S.; Zecchina, A. Infrared Spectroscopy of Surface Transient Species. *Adv. Catal.* **2007**, *51*, 1−74.

(12) Lamberti, C.; Zecchina, A.; Groppo, E.; Bordiga, S. Probing the Surfaces of Heterogeneous Catalysts by in Situ IR Spectroscopy. *Chem. Soc. Rev.* **2010**, *39*, 4951−5001.

(13) Vimont, A.; Thibault-Starzyk, F.; Daturi, M. Analysing and Understanding the Active Site by IR Spectroscopy. *Chem. Soc. Rev.* **2010**, *39*, 4928−4950.

(14) Zhu, H.; Kwak, J. H.; Peden, C. H. F.; Szanyi, J. In Situ DRIFT-MS Studies on the Oxidation of Adsorbed NH_3 by NO_x over a Cu-SSZ-13 Zeolite. *Catal. Today* **2013**, *205*, 16−23.
(15) Wang, D.; Zhang, L.; Kamasamudram, K.; Epling, W. S. In Situ-DRIFTS Study of Selective Catalytic Reduction of NO_x by NH_3 over Cu-Exchanged SAPO-34. *ACS Catal.* **2013**, *3*, 871−881.
(16) Sjövall, H.; Fridell, E.; Blint, R. J.; Olsson, L. Identification of Adsorbed Species on Cu-ZSM-5 under NH_3 SCR Conditions. *Top. Catal.* **2007**, *42*, 113−117.
(17) Lezcano-Gonzalez, I.; Deka, U.; Arstad, B.; Van Yperen-De Deyne, A.; Hemelsoet, K.; Waroquier, M.; Van Speybroeck, V.; Weckhuysen, B. M.; Beale, A. M. Determining the Storage, Availability and Reactivity of NH_3 within Cu-Chabazite-Based Ammonia Selective Catalytic Reduction Systems. *Phys. Chem. Chem. Phys.* **2014**, *16*, 1639−1650.
(18) Zecchina, A.; Marchese, L.; Bordiga, S.; Paze, C.; Gianotti, E. Vibrational Spectroscopy of NH_4^+ Ions in Zeolitic Materials: An IR Study. *J. Phys. Chem. B* **1997**, *101*, 10128−10135.
(19) Datka, J.; Gora-Marek, K. IR Studies of the Formation of Ammonia Dimers in Zeolites TON. *Catal. Today* **2006**, *114*, 205−210.
(20) Lonyi, F.; Valyon, J. On the Interpretation of the NH_3-TPD Patterns of H-ZSM-5 and H-Mordenite. *Microporous Mesoporous Mater.* **2001**, *47*, 293−301.
(21) Bordiga, S.; Groppo, E.; Agostini, G.; van Bokhoven, J. A.; Lamberti, C. Reactivity of Surface Species in Heterogeneous Catalysts Probed by in Situ X-Ray Absorption Techniques. *Chem. Rev.* **2013**, *113*, 1736−1850.
(22) Mino, L.; Agostini, G.; Borfecchia, E.; Gianolio, D.; Piovano, A.; Gallo, E.; Lamberti, C. Low-Dimensional Systems Investigated by X-Ray Absorption Spectroscopy: A Selection of 2D, 1D and 0D Cases. *J. Phys. D: Appl. Phys.* **2013**, *46*, 423001.
(23) Singh, J.; Lamberti, C.; van Bokhoven, J. A. Advanced X-Ray Absorption and Emission Spectroscopy: In Situ Catalytic Studies. *Chem. Soc. Rev.* **2010**, *39*, 4754−4766.
(24) Korhonen, S. T.; Fickel, D. W.; Lobo, R. F.; Weckhuysen, B. M.; Beale, A. M. Isolated Cu^{2+} Ions: Active Sites for Selective Catalytic Reduction of NO. *Chem. Commun.* **2011**, *47*, 800−802.
(25) Deka, U.; Juhin, A.; Eilertsen, E. A.; Emerich, H.; Green, M. A.; Korhonen, S. T.; Weckhuysen, B. M.; Beale, A. M. Confirmation of Isolated Cu^{2+} Ions in SSZ-13 Zeolite as Active Sites in NH_3-Selective Catalytic Reduction. *J. Phys. Chem. C* **2012**, *116*, 4809−4818.
(26) McEwen, J. S.; Anggara, T.; Schneider, W. F.; Kispersky, V. F.; Miller, J. T.; Delgass, W. N.; Ribeiro, F. H. Integrated Operando X-Ray Absorption and DFT Characterization of Cu-SSZ-13 Exchange Sites During the Selective Catalytic Reduction of NO_x with NH_3. *Catal. Today* **2012**, *184*, 129−144.
(27) Woertink, J. S.; Smeets, P. J.; Groothaert, M. H.; Vance, M. A.; Sels, B. F.; Schoonheydt, R. A.; Solomon, E. I. A $[Cu_2O]^{2+}$ Core in Cu-ZSM-5, the Active Site in the Oxidation of Methane to Methanol. *Proc. Natl. Acad. Sci. U.S.A.* **2009**, *106*, 18908−18913.
(28) Giordanino, F.; Vennestrom, P. N. R.; Lundegaard, L. F.; Stappen, F. N.; Mossin, S. L.; Beato, P.; Bordiga, S.; Lamberti, C. Characterization of Cu-Exchanged SSZ-13: A Compared FTIR, UV-Vis and EPR Study with Cu-ZSM-5 and Cu-β with Similar Si/Al and Cu/Al Ratios. *Dalton Trans.* **2013**, *42*, 12741−12761.
(29) Salmon, P. S.; Neilson, G. W.; Enderby, J. E. The Structure of Cu^{2+} Aqueous-Solutions. *J. Phys. C* **1988**, *21*, 1335−1349.
(30) Benfatto, M.; D'Angelo, P.; Della Longa, S.; Pavel, N. V. Evidence of Distorted Fivefold Coordination of the Cu^{2+} Aqua Ion from an X-Ray-Absorption Spectroscopy Quantitative Analysis. *Phys. Rev. B* **2002**, *65*, 174205.
(31) Larsen, S. C.; Aylor, A.; Bell, A. T.; Reimer, J. A. Electron Paramagnetic Resonance Studies of Copper Ion-Exchanged ZSM-5. *J. Phys. Chem.* **1994**, *98*, 11533−11540.
(32) Palomino, G. T.; Bordiga, S.; Zecchina, A.; Marra, G. L.; Lamberti, C. XRD, XAS, and IR Characterization of Copper-Exchanged Y Zeolite. *J. Phys. Chem. B* **2000**, *104*, 8641−8651.
(33) Alayon, E. M. C.; Nachtegaal, M.; Bodi, A.; van Bokhoven, J. A. Reaction Conditions of Methane-to-Methanol Conversion Affect the Structure of Active Copper Sites. *ACS Catal.* **2014**, *4*, 16−22.
(34) Llabrés i Xamena, F. X.; Fisicaro, P.; Berlier, G.; Zecchina, A.; Palomino, G. T.; Prestipino, C.; Bordiga, S.; Giamello, E.; Lamberti, C. Thermal Reduction of Cu^{2+} Mordenite and Re-Oxidation Upon Interaction with H_2O, O_2, and NO. *J. Phys. Chem. B* **2003**, *107*, 7036−7044.
(35) Kau, L. S.; Spirasolomon, D. J.; Pennerhahn, J. E.; Hodgson, K. O.; Solomon, E. I. X-Ray Absorption-Edge Determination of the Oxidation-State and Coordination-Number of Copper - Application to the Type-3 Site in Rhus-Vernicifera Laccase and Its Reaction with Oxygen. *J. Am. Chem. Soc.* **1987**, *109*, 6433−6442.
(36) Sano, M.; Komorita, S.; Yamatera, H. Xanes Spectra of Copper(II) Complexes - Correlation of the Intensity of the 1s-3d Transition and the Shape of the Complex. *Inorg. Chem.* **1992**, *31*, 459−463.
(37) Lamberti, C.; Bordiga, S.; Salvalaggio, M.; Spoto, G.; Zecchina, A.; Geobaldo, F.; Vlaic, G.; Bellatreccia, M. XAFS, IR, and UV-Vis Study of the Cu-I Environment in Cu-I-ZSM-5. *J. Phys. Chem. B* **1997**, *101*, 344−360.
(38) Groothaert, M. H.; van Bokhoven, J. A.; Battiston, A. A.; Weckhuysen, B. M.; Schoonheydt, R. A. Bis (μ−Oxo) Dicopper in Cu-ZSM-5 and Its Role in the Decomposition of NO: A Combined in Situ XAFS, UV-Vis-near-IR, and Kinetic Study. *J. Am. Chem. Soc.* **2003**, *125*, 7629−7640.
(39) Kervinen, K.; Bruijnincx, P. C. A.; Beale, A. M.; Mesu, J. G.; van Koten, G.; Gebbink, R.; Weckhuysen, B. M. Zeolite Framework Stabilized Copper Complex Inspired by the 2-His-1-Carboxylate Facial Triad Motif Yielding Oxidation Catalysts. *J. Am. Chem. Soc.* **2006**, *128*, 3208−3217.
(40) Tranquada, J. M.; Heald, S. M.; Moodenbaugh, A. R. X-Ray-Absorption near-Edge-Structure Study of $La_{2-X}(Ba,Sr)_XCuO_{4-Y}$ Superconductors. *Phys. Rev. B* **1987**, *36*, 5263−5274.
(41) Prestipino, C.; Berlier, G.; Xamena, F.; Spoto, G.; Bordiga, S.; Zecchina, A.; Palomino, G. T.; Yamamoto, T.; Lamberti, C. An in Situ Temperature Dependent IR, EPR and High Resolution Xanes Study on the NO/Cu^+-ZSM-5 Interaction. *Chem. Phys. Lett.* **2002**, *363*, 389−396.
(42) Palomino, G. T.; Fisicaro, P.; Bordiga, S.; Zecchina, A.; Giamello, E.; Lamberti, C. Oxidation States of Copper Ions in ZSM-5 Zeolites. A Multitechnique Investigation. *J. Phys. Chem. B* **2000**, *104*, 4064−4073.
(43) Kau, L. S.; Hodgson, K. O.; Solomon, E. I. X-Ray Absorption Edge and EXAFS Study of the Copper Sites in Zinc Oxide Methanol Synthesis Catalysts. *J. Am. Chem. Soc.* **1989**, *111*, 7103−7109.
(44) Koebel, M.; Elsener, M.; Kleemann, M. Urea-SCR: A Promising Technique to Reduce NO_x Emissions from Automotive Diesel Engines. *Catal. Today* **2000**, *59*, 335−345.
(45) Pazé, C.; Bordiga, S.; Lamberti, C.; Salvalaggio, M.; Zecchina, A.; Bellussi, G. Acidic Properties of H-Beta Zeolite as Probed by Bases with Proton Affinity in the 118−204 kcal Mol^{-1} Range: A FTIR Investigation. *J. Phys. Chem. B* **1997**, *101*, 4740−4751.
(46) Bordiga, S.; Regli, L.; Cocina, D.; Lamberti, C.; Bjorgen, M.; Lillerud, K. P. Assessing the Acidity of High Silica Chabazite H-SSZ-13 by FTIR Using CO as Molecular Probe: Comparison with H-SAPO-34. *J. Phys. Chem. B* **2005**, *109*, 2779−2784.
(47) Bordiga, S.; Roggero, I.; Ugliengo, P.; Zecchina, A.; Bolis, V.; Artioli, G.; Buzzoni, R.; Marra, G.; Rivetti, F.; Spano, G.; Lamberti, C. Characterisation of Defective Silicalites. *J. Chem. Soc., Dalton Trans.* **2000**, 3921−3929.
(48) Bonelli, B.; Zanzottera, C.; Armandi, M.; Esposito, S.; Garrone, E. IR Spectroscopic Study of the Acidic Properties of Alumino-Silicate Single-Walled Nanotubes of the Imogolite Type. *Catal. Today* **2013**, *218−219*, 3−9.
(49) Lamberti, C.; Morterra, C.; Bordiga, S.; Cerrato, G.; Scarano, D. Band Resolution Techniques and Fourier-Transform Infrared-Spectra of Adsorbed Species. *Vib. Spectrosc.* **1993**, *4*, 273−284.

(50) Glatzel, P.; Weng, T.-C.; Kvashnina, K.; Swarbrick, J.; Sikora, M.; Gallo, E.; Smolentsev, N.; Mori, R. A. Reflections on Hard X-Ray Photon-in/Photon-out Spectroscopy for Electronic Structure Studies. *J. Electron Spectrosc. Relat. Phenom.* **2013**, *188*, 17−25.
(51) Lamble, G.; Moen, A.; Nicholson, D. G. Structure of the Diamminecopper(I) Ion in Solution. An X-Ray Absorption Spectroscopic Study. *J. Chem. Soc., Faraday Trans.* **1994**, *90*, 2211−2213.
(52) Mathisen, K.; Stockenhuber, M.; Nicholson, D. G. In Situ XAS and IR Studies on Cu:SAPO-5 and Cu:SAPO-11: The Contributory Role of Monomeric Linear Copper(I) Species in the Selective Catalytic Reduction of NO_x by Propene. *Phys. Chem. Chem. Phys.* **2009**, *11*, 5476−5488.
(53) Gomez-Lor, B.; Iglesias, M.; Cascales, C.; Gutierrez-Puebla, E.; Monge, M. A. A Diamine Copper(I) Complex Stabilized in Situ within the Ferrierite Framework. Catalytic Properties. *ACS Chem. Mater.* **2001**, *13*, 1364−1368.
(54) Gallo, E.; Lamberti, C.; Glatzel, P. Investigation of the Valence Electronic States of Ti(IV) in Ti Silicalite-1 Coupling X-Ray Emission Spectroscopy and Density Functional Calculations. *Phys. Chem. Chem. Phys.* **2011**, *13*, 19409−19419.
(55) Gallo, E.; Bonino, F.; Swarbrick, J. C.; Petrenko, T.; Piovano, A.; Bordiga, S.; Gianolio, D.; Groppo, E.; Neese, F.; Lamberti, C.; Glatzel, P. Preference Towards Five-Coordination in Ti Silicalite-1 Upon Molecular Adsorption. *ChemPhysChem* **2013**, *14*, 79−83.
(56) Glatzel, P.; Bergmann, U. High Resolution 1s Core Hole X-Ray Spectroscopy in 3d Transition Metal Complexes - Electronic and Structural Information. *Coord. Chem. Rev.* **2005**, *249*, 65−95.
(57) Vegelius, J. R.; Kvashnina, K. O.; Klintenberg, M.; Soroka, I. L.; Butorin, S. M. Cu $K\beta_{2,5}$ X-Ray Emission Spectroscopy as a Tool for Characterization of Monovalent Copper Compounds. *J. Anal. At. Spectrom.* **2012**, *27*, 1882−1888.
(58) *ADF2012*; SCM, Theoretical Chemistry, Vrije Universiteit: Amsterdam, The Netherlands, 2012. http://www.scm.com.
(59) te Velde, G.; Bickelhaupt, F. M.; Baerends, E. J.; Guerra, C. F.; Van Gisbergen, S. J. A.; Snijders, J. G.; Ziegler, T. Chemistry with ADF. *J. Comput. Chem.* **2001**, *22*, 931−967.
(60) Busca, G.; Lietti, L.; Ramis, G.; Berti, F. Chemical and Mechanistic Aspects of the Selective Catalytic Reduction of NO_x by Ammonia over Oxide Catalysts: A Review. *Appl. Catal., B* **1998**, *18*, 1−36.
(61) Pant, A.; Schmieg, S. J. Kinetic Model of NO_x SCR Using Urea on Commercial Cu-Zeolite Catalyst. *Ind. Eng. Chem.* **2011**, *50*, 5490−5498.
(62) Davydov, A. The Nature of Oxide Surface Centers. In *Molecular Spectroscopy of Oxide Catalyst Surfaces*; John Wiley & Sons, Ltd.: Chichester, U.K., 2003; pp 27−179.
(63) Peri, J. B. Infrared Study of OH and NH_2 Groups on the Surface of a Dry Silica Aerogel. *J. Phys. Chem.* **1966**, *70*, 2937−2945.
(64) Folman, M. Infra-Red Studies of NH_3 Adsorption on Chlorinated Porous Vycor Glass. *Trans. Faraday Soc.* **1961**, *57*, 2000−2006.
(65) Coluccia, S.; Garrone, E.; Borello, E. Infrared Spectroscopic Study of Molecular and Dissociative Adsorption of Ammonia on Magnesium Oxide, Calcium Oxide and Strontium Oxide. *J. Chem. Soc., Faraday Trans. 1* **1983**, *79*, 607−613.
(66) Larrubia, M. A.; Ramis, G.; Busca, G. An FT-IR Study of the Adsorption of Urea and Ammonia over V_2O_5-MoO_3-TiO_2 SCR Catalysts. *Appl. Catal. B: Environ.* **2000**, *27*, L145−L151.
(67) Szanyi, J.; Kwak, J. H.; Zhu, H.; Peden, C. H. F. Characterization of Cu-SSZ-13 NH_3 SCR Catalysts: An in Situ FTIR Study. *Phys. Chem. Chem. Phys.* **2013**, *15*, 2368−2380.
(68) Spoto, G.; Zecchina, A.; Bordiga, S.; Ricchiardi, G.; Martra, G.; Leofanti, G.; Petrini, G. Cu(I)-ZSM-5 Zeolites Prepared by Reaction of H-ZSM-5 with Gaseous CuCl: Spectroscopic Characterization and Reactivity Towards Carbon Monoxide and Nitric Oxide. *Appl. Catal., B* **1994**, *3*, 151−172.
(69) Bolis, V.; Maggiorini, S.; Meda, L.; D'Acapito, F.; Turnes Palomino, G.; S. Bordiga, S.; Lamberti, C. X-ray Photoelectron Spectroscopy and X-ray Absorption Near Edge Structure Study of Copper Sites Hosted at the Internal Surface of ZSM-5 Zeolite: A Comparison with Quantitative and Energetic Data on the CO and NH_3 Adsorption. *J. Chem. Phys.* **2000**, *113*, 9248−9261.